Nonlinear current of strongly irradiated quantum Hall gas

Assa Auerbach and G. Venketeswara Pai
Physics Department, Technion, Haifa 32000, Israel
(Received 23 September 2007; published 20 November 2007)

Two dimensional electrons in weakly disordered high Landau levels are considered. The current-field response in the presence of a strong microwave field is computed. The *disordered Floquet evolution operator* allows us to treat the short range disorder perturbatively, at any strength of electric fields. A simplifying *random matrix approximation* reproduces the broadened Landau level density of states and structure factor. We derive the magnitude of the microwave induced resistivity oscillations. The disorder short wavelength cutoff determines the nonlinear electric fields of the zero resistance state and the Hall induced resistivity oscillations. We discuss wider implications of our results on experiments and other theories.

DOI: 10.1103/PhysRevB.76.205318 PACS number(s): 73.40.−c, 73.43.Qt, 73.50.Fq, 73.50.Pz

I. INTRODUCTION

Some remarkable phenomena have been recently observed in high mobility GaAs/AlGaAs heterostructures: microwave induced resistance oscillations (MIROs), zero resistance states (ZRSs),[1–5] and Hall induced resistivity oscillations (HIROs).[6–10] These experiments are carried out at weak fields (relative to the quantum Hall regime) and at temperatures $T \geqslant \hbar\omega_c$ (ω_c is the cyclotron frequency), where Shubnikov–de Haas oscillations are thermally smeared. Nevertheless, microwave radiation, or large Hall currents, can expose the underlying Landau quantization via the MIRO and HIRO oscillations.

MIRO (in the Hall bar geometry) exhibits large magnetoresistance oscillations as a function of radiation frequency ω, with nodes at harmonics of $m\omega_c$, $m=1,2,\ldots$. In strong enough radiation, the resistance in the positive detuning regimes may be nearly completely suppressed. This phenomenon is commonly denoted ZRS. The ZRS has been attributed to the spontaneous generation of internal electric field domains.[11] The macroscopic structure and stability of ZRS domains have been investigated by a phenomenological Lyapunov functional.[12,13]

Microscopic theories for MIRO and ZRS are divided into two categories. (i) The displacement photocurrent (DP) mechanism which was proposed by Ryzhii *et al.*[14] and Durst *et al.*[15] See also Refs. 16, 17, and 19. The DP is stronger for well resolved Landau levels, whose width Γ is smaller than the Landau level separation $\hbar\omega_c$. (ii) The distribution function (DF) mechanism was proposed by Dmitriev *et al.*[18] and Vavilov and Aleiner.[19] The DF mechanism becomes important when the inelastic lifetime is much longer than the elastic transport scattering time.

Independent of the particular dominant mechanism, the disorder potential is essential for the dissipative currents. Treating disorder in high Landau levels is an old theoretical challenge: since the clean system has macroscopic Landau level degeneracies, a straightforward perturbation theory in disorder is ill posed. The *linear, dark conductivity* (in the absence of radiation) has been calculated by the self-consistent Born approximation (SCBA).[20,21] The SCBA is a selective diagram resummation, whose neglected vertex corrections are controlled by the smoothness of the disorder.[22] Unfortunately, a controlled extension of the SCBA to strong static and time dependent fields has so far proven difficult. Nevertheless, the ZRS and the HIRO are inherently nonlinear effects which require theoretical attention.

In this paper, we devise a "divide and conquer" method,[23] which incorporates strong electric fields with the disorder potential. It has long been appreciated that strong radiation effects on the *clean* Landau levels are tractable using a *Floquet transformation*.[14,17] However, writing down an explicit Floquet transformation for a disordered Hamiltonian is, in general, intractable. Here, we make progress by exploiting the commutation between Landau and guiding center operators. We construct a separable disordered Hamiltonian, which is completely "Floquet transformable." This trick allows us to eliminate the electric fields and obtain the random Floquet (quasistationary) eigenfunctions. These states describe our zeroth order density matrix, without any dissipative current. The dissipative current is subsequently computed perturbatively, to leading order in the remainder short wavelength disorder. The physical small parameter is the ratio of transport scattering rate to Landau level width.

This approach allows us to answer some outstanding questions.

(1) What is optimal disorder for large MIRO and ZRS effects? We identify the "figure of merit" as the ratio $R=\hbar\omega_c/\Gamma$, which is also expected to be large in systems exhibiting the HIRO effect.

(2) What characteristic Hall fields determine the HIRO effect? The low intraband field is

$$E_\Gamma = \Gamma/(el_B^2 q_s), \tag{1}$$

and the higher "interband" field periodicity is given by

$$E_{\omega_c} = \hbar\omega_c/(el_B^2 q_s), \tag{2}$$

where q_s is the high wave-vector cutoff of the disorder fluctuations and l_B is the Landau length.

(3) What is the expected magnitude of the spontaneous ZRS fields? The quantity E_Γ sets the overall scale of the ZRS field E^{zrs}, which also depends on R, frequency, and microwave power. E^{zrs} has a second order dynamical phase transition at a threshold microwave power.

This paper is organized as follows. Section II briefly reviews the macroscopic transport theory of the Corbino and Hall bar geometries. The main purpose is to define the *dissipative current*, which is the subject of subsequent sections. Section III introduces the microscopic model: noninteracting electrons in a weak magnetic field, with "broad-tail" disorder correlations. The disorder potential is split into two operators, where the long wavelength components are (mostly) incorporated into the broadened Landau levels Hamiltonian. In Sec. IV, the disordered Floquet evolution operator $U_d(t)$ is constructed. We show that while the Landau levels broaden into random Floquet eigenstates, the dc field (surprisingly) produces no dissipative current and a perfect classical Hall current. The random matrix approximation (RMA) captures the spectrum and eigenfunctions of the broadened Landau levels and recovers the well known SCBA. In Sec. V, we derive the leading order dissipative nonlinear current [Eq. (48)], which can be disorder averaged numerically. In Sec. VI, the current formula is simplified by the RMA to a tractable analytical expression [Eq. (59)]. The simplified expression is analyzed in some detail: the SCBA dark conductivity is recovered, and the MIRO, ZRS, and HIRO effects are obtained. Predictions are obtained for the magnitudes of these effects and the values of nonlinear field scales. A plot of the full microwave irradiated current as a function of dc field is given in Fig. 9. We conclude with a brief discussion of theoretical and experimental issues pertinent to our results. Appendix A calculates the disorder matrix elements and Appendix B derives the explicit Floquet operator.

II. MACROSCOPIC TRANSPORT THEORY

Here, we briefly review the magnetotransport theory of the Corbino and Hall bar geometries. This will provide a direct relation between the experimentally measurable currents and voltages and the quantity calculated theoretically in later sections: *the nonlinear dissipative current* $j^d(E)$.

In the presence of a microwave field $\mathbf{E}_\omega$ and a dc field $\mathbf{E}=E\hat{\mathbf{E}}$, macroscopic transport theory assumes a *local* relation between the dc current density and the electric field,

$$\mathbf{j} = j^d(E,\mathbf{E}_\omega)\hat{\mathbf{E}} + \mathbf{j}^H(\mathbf{E}),$$

$$\mathbf{j}^H = \sigma_H \hat{\mathbf{z}} \times \mathbf{E}, \tag{3}$$

where $\mathbf{j}^H$ is the nondissipative Hall current and σ_H is the Hall conductivity. σ_H and $j^d(E)$ require input from a microscopic theory, which involve quantum mechanical scattering processes on length scales shorter than the inelastic dephasing length.

In the presence of large scale inhomogeneities (considered in Refs. 12 and 13), the dissipative current $\mathbf{j}^d(\mathbf{r})$ is not necessarily parallel to $\mathbf{E}(\mathbf{r})$ and σ_H may vary in space. Here, we do not consider such large scale disorder.

A. Corbino geometry

By the definition [Eq. (3)], for a position independent σ_H, the dissipative and Hall currents are conserved separately,

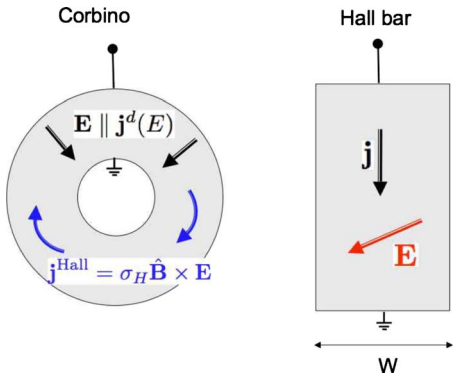

FIG. 1. (Color online) Definition of currents in the Corbino and Hall bar geometries. In the homogeneous Corbino sample, the electric field and dissipative current density are radial, while the nondissipative Hall current is azimuthal. In the Hall bar, the vertical current between leads includes both dissipative and nondissipative components. For large Hall angle $\sigma_H \gg \sigma_{xx}$, most (but not all) of the current is nondissipative.

$$\nabla \cdot \mathbf{j} = \nabla \cdot \mathbf{j}^H = \nabla \cdot (j^d \hat{\mathbf{E}}) = 0. \tag{4}$$

In a Corbino geometry (see Fig. 1), one specifies the potential on the inner and outer boundaries of the sample, which determines the purely radial electric field $\mathbf{E}=E(r)\hat{\mathbf{r}}$. The dissipative current $\mathbf{j}^d$ is also radial, while the nondissipative Hall current circulates around the annulus unrestricted.

The Corbino geometry completely separates the effects of σ_H and $\mathbf{j}^d$ and is simpler to analyze theoretically. The function $j^d(E)$ is uniquely determined for particular sample dimensions, from the total current and voltage between the outer and inner edges, with no dependence on σ_H.

As was shown in Refs. 11–13, in the absence of an external bias current, a negative conductivity in some field range $j^d(E)<0$ may be unstable to spontaneously created domains of finite internal fields whose magnitudes are $|\mathbf{E}|=E^{zrs}$ and orientation is determined by the boundary conditions and long range potentials,

$$j^d(E^{zrs}) = 0. \tag{5}$$

In the absence of "pinning" in the Lyapunov functional, the domain walls are free to move and absorb any charge in external bias voltage, leaving the current vanishingly small. This is the so-called ZRS, which, confusingly, yields zero *conductance* in the Corbino geometry.

B. Hall bar geometry

Experimentally, the Hall bar geometry (see Fig. 1) is more popular for ease of fabrication. The Hall bar geometry imposes $j_y=0$. The current is forced through in one direction $\mathbf{j}=j\hat{\mathbf{x}}$, and the longitudinal and transverse voltage drops are measured. The electrochemical field $\mathbf{E}=(E_x,E_y)$ can be deduced from the geometry. By Eq. (3), the electric field satisfies the coupled nonlinear equations

$$j = j^d(E)\frac{E_x}{E} + \sigma_H E_y,$$

$$0 = -\sigma_H E_x + j^d(E)\frac{E_y}{E}. \tag{6}$$

In the case of large Hall angle,

$$\sigma_H \gg \sigma_{xx} \equiv j^d/E, \tag{7}$$

and thus $E \approx E_y \gg E_x$. This inequality simplifies the solution of Eq. (6),

$$E_y(j) \approx \frac{j^d(E)}{\sigma_H}[1 + \mathcal{O}(|\sigma_{xx}|/\sigma_H)], \tag{8}$$

where we can drop the terms of order $\sigma_{xx}/\sigma_H \ll 1$. An experimental measurement of $E_x(j)$ approximately describes the nonlinear function $j^d(E)$, which will be calculated in Eq. (48),

$$E_x(j) \approx \frac{1}{\sigma_H} j^d\left(\frac{j}{\sigma_H}\right). \tag{9}$$

The negative conductivity implies $\mathbf{E}\cdot\mathbf{j} < 0$. In the ZRS, the spontaneous fields E^{zrs} of Eq. (5) are associated with the dissipationless flow of Hall currents with magnitude

$$|j^{zrs}| = \sigma_H E^{zrs}. \tag{10}$$

In the ZRS, the currents traverse the system in the x direction, producing very little longitudinal voltage drop and dissipation. For the Hall bar geometry of width W (see Fig. 1), the resistivity remains vanishingly small up to a critical current I^{cr} given by

$$I^{cr} = W\sigma_H E^{zrs}. \tag{11}$$

Thus, the critical current directly measures the internal ZRS field.

III. MICROSCOPIC MODEL

We consider a two dimensional electron gas (2DEG) subject to a perpendicular magnetic field $B\hat{\mathbf{z}}$, microwave field $\mathbf{E}_\omega$, and a dc field $\mathbf{E}_{dc}$. The standard treatment of electrons in a magnetic field defines the dimensionless Landau level and guiding center coordinates as

$$\boldsymbol{\pi} \equiv \frac{l_B}{\hbar}\mathbf{p} + \frac{1}{2l_B}\hat{\mathbf{z}} \times \mathbf{r},$$

$$\mathbf{R} \equiv \frac{\mathbf{r}}{2l_B} + \frac{l_B}{\hbar}\hat{\mathbf{z}} \times \mathbf{p}, \tag{12}$$

where the magnetic length is $l_B = \sqrt{\hbar c/eB}$. By construction, the two guiding center components commute with the two Landau operators

$$[\pi^\alpha, R^\beta] = 0, \quad \alpha, \beta = x, y. \tag{13}$$

The microscopic model Hamiltonian is

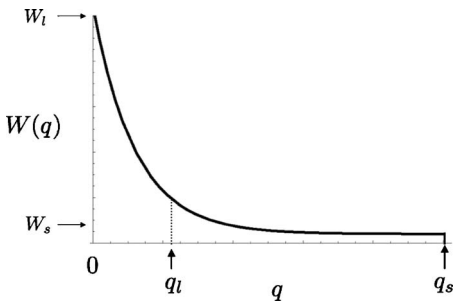

FIG. 2. The broad-tail model of disorder correlations of Eq. (18). The wave vector q_l bounds the long wavelength spectrum, which is incorporated into the disordered Floquet evolution operator (see text). Most of the spectral weight is below q_l, although the higher moments which determine the dissipative current are dominated by the short wavelength cutoff q_s.

$$\mathcal{H}(t) = \frac{\hbar\omega_c}{2}|\boldsymbol{\pi} + \mathbf{a}(t)|^2 + \mathcal{V}(\mathbf{r}), \tag{14}$$

where $\omega_c = eB/(mc)$ is the cyclotron frequency. The electric fields are represented by the dimensionless gauge field

$$\mathbf{a}(t) = \frac{el_B}{\hbar}\left(\Re\left[\frac{\mathbf{E}_\omega}{\omega}e^{-i\omega t}\right] + \mathbf{E}_{dc}t\right). \tag{15}$$

The disorder potential is described by a random function of position $\mathbf{r}$,

$$\mathcal{V} = \frac{1}{\mathcal{A}}\sum_{\mathbf{q}} V_{\mathbf{q}} e^{-i\mathbf{q}\cdot\mathbf{r}}, \tag{16}$$

where $\mathcal{A}$ is the area of the system. The Fourier components are random complex numbers obeying $V_{\mathbf{q}} = V^*_{-\mathbf{q}}$, with correlations

$$\langle V_{\mathbf{q}} V_{-\mathbf{q}'}\rangle = \mathcal{A}W(q)\delta_{\mathbf{q},\mathbf{q}'}. \tag{17}$$

Our *divide and conquer* tactic is to split the disorder potential into two components by a dividing wave vector q_l. We assume that $W(q)$ is a *broad-tail distribution* (see Fig. 2), i.e., most of its weight is concentrated in a region below some dividing wave vector q_l (say, of the order of l_B), but the higher *moments* are dominated by much shorter wavelengths. For example, we might choose the function

$$W(q) = W_l e^{-2q/q_l} + W_s\theta(q_s - q),$$

$$\frac{q_l}{q_s} < \frac{W_s q_s}{W_l q_l} < 1, \tag{18}$$

such as depicted in Fig. 2.

This model is realistic for high mobility heterostructures, where the offset distance to unscreened charges is $d = 1/q_l$,[24] and W_s is the intrinsic short range disorder of the 2DEG. The upper cutoff is effectively at some $q_s \leqslant \pi k_F$. We do not include at this level any electron-phonon or electron-electron interactions.

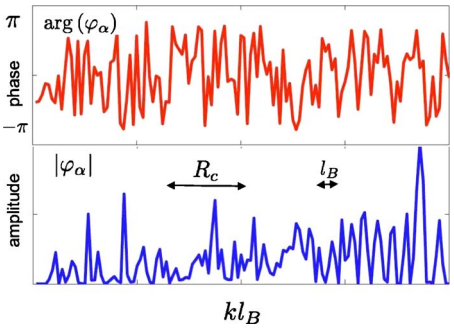

FIG. 3. (Color online) A typical numerically computed eigenstate φ_α, chosen closest to the band center. The phase (amplitude) is plotted in the top (bottom) panel. kl_B describes the height position on the cylinder. We use Landau degeneracy $n_L=128$, Fermi level $n_F=15$, and cutoff $q_l=2/l_B$ for the long range disorder. The cyclotron radius and Landau length are depicted.

A. Splitting the disorder

The main trick is to split the disorder into two operators

$$\mathcal{V}(\mathbf{r}) = \mathcal{V}_l(\mathbf{R}) + \mathcal{V}_s(\boldsymbol{\pi},\mathbf{R}). \tag{19}$$

The long wavelength disorder term is *defined* as the operator

$$\mathcal{V}_l \equiv \sum_{nkk'} V^{n_F}_{kk'} |nk\rangle\langle nk'| = \sum_{n\alpha} \epsilon_\alpha |n\alpha\rangle\langle n\alpha|, \tag{20}$$

where n_F is the single-spin filling factor at the Fermi energy. The Landau level degeneracy is $n_L=\mathcal{A}/(2\pi l_B^2)$, where $\mathcal{A}$ is the system area. Without loss of generality, we choose the basis $|nk\rangle$ on a cylinder of circumference $L_x=\sqrt{\mathcal{A}}$, where n is the Landau level index and $k=2\pi m l_B/L_x$, where $m=1,\ldots n_L$. The state $|k\rangle$ is centered at position $\langle y\rangle=kl_B$. The matrix elements of $\mathcal{V}_l$ are the (identical) block-diagonal matrices (see Appendix A),

$$V^{n_F}_{kk'} = \frac{1}{\mathcal{A}} \sum_{|\mathbf{q}|\leqslant q_l} V_{\mathbf{q}} e^{-\tilde{q}^2/4} L_{n_F}\left(\frac{\tilde{q}^2}{2}\right) e^{-i\tilde{q}_x[(k+k')/2]} \delta_{k+\tilde{q}_y,k'}, \tag{21}$$

where L_n is the Laguerre polynomial of order n and $\tilde{q}\equiv q l_B$. In Eq. (20), ϵ_α and $\varphi_\alpha(k)=\langle k|n\alpha\rangle$ are the disordered spectrum and eigenvectors, respectively.

$\mathcal{V}_l$, by construction, has no interband matrix elements and identical intraband blocks. It is therefore a random function of *only* the guiding center operators $\mathbf{R}$ [see Eq. (12)]. Nevertheless, it contains most of the spectral weight of the disorder.

B. Random matrix approximation

We shall now see that at high Landau levels, $V^{n_F}_{kk'}$ is well represented by a random Hermitian matrix. Its eigenstates appear as random extended wave functions, as depicted in Fig. 3.

Although numerical averaging over disorder poses no great difficulty, the statistical properties of $V^{n_F}_{kk'}$ suggest to approximate it as a Hermitian random matrix of the Gaussian unitary ensemble (GUE). This RMA will provide easy averaging of spectra and correlations over the long wavelength disorder. This presents another example of the usefulness of the random matrix theory[26] for quantum transport.[27]

Fortunately, the RMA becomes exact in the limit of a uniform white-noise disorder fluctuation $W(q)=W$ and large filling factor. The matrix elements of $V^{n_F}_{kk'}$ become maximally uncorrelated,

$$\lim_{n_F\to\infty} \langle \mathcal{V}^{n_F}_{kk'} \mathcal{V}^{n_F}_{k''k'''} \rangle_{V_{\mathbf{q}}} = \frac{1}{\pi R_c \mathcal{A}} \sum_{\mathbf{q}} \frac{W(q)}{\sqrt{qq'}} e^{i\tilde{q}_x(k-k''')} \delta_{k',k+\tilde{q}_y} \delta_{k'',k'''+\tilde{q}_y}$$

$$\approx \left(\frac{2\pi l_B^2}{\mathcal{A}}\right) \Gamma_{RMA} \delta_{k,k'''} \delta_{k',k''},$$

$$\Gamma^2_{RMA} = \frac{1}{2\pi^2 R_c} \int_0^\infty dq W(q), \tag{22}$$

where $R_c=l_B\sqrt{2n_F}$. The density of states is defined as an ensemble average

$$\nu(E) = \left\langle \sum_{n\alpha} \delta(E-E_{n\alpha}) \right\rangle_{\mathcal{V}_l}. \tag{23}$$

For a GUE ensemble, the density of states of each Landau band is expected to be semielliptical. In the limit of narrow Landau levels, the SCBA also produces semielliptical density of states. Moreover, the SCBA[20,22] for the Landau level broadening (sometimes called in the literature "quasiparticle scattering rate" $\hbar/\tau_s$) equals Γ_{RMA}, within the assumptions of Eq. (18).

Here, however, we are interested in the long range disorder where $q_l \ll k_F < \infty$. This implies that the matrix elements of $V^{n_F}_{kk'}$ are correlated within a distance $\Delta k \leqslant 1/(l_B q_l)$ and that the density of states at the tails will not be well described by the RMA's semielliptical form.

In the regime $q_l l_B \in [0.3,5]$, the numerical density of states, averaged over a Gaussian distribution of disorder potentials $\{V_{\mathbf{q}}\}$, can be fitted to a sum of Gaussians,

$$\nu(E) \simeq \frac{1}{(2\pi)^{3/2} l_B^2 \Gamma} \sum_n e^{-(E-n\hbar\omega_c)^2/2\Gamma^2}. \tag{24}$$

As shown in Fig. 4, the Gaussian fit is excellent for $q_l l_B=2$. The fitted Landau level width Γ is also quite close to the RMA result,

$$\Gamma \approx 1.3\Gamma^{RMA}. \tag{25}$$

The RMA for the eigenfunction correlations, which determine the structure factor, will be investigated later in Sec. V D.

IV. FLOQUET TRANSFORMATION OF TIME DEPENDENT FIELDS

A. Clean Landau levels

The clean Hamiltonian, driven by a time dependent vector potential, is

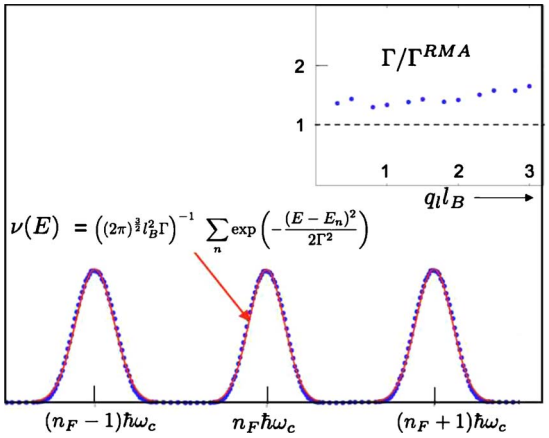

FIG. 4. (Color online) Numerical averaging of 500 disorder potentials, for the density of states $\rho(\epsilon)$ of $V_{kk'}^{n_F}$, using $W_l=l_B^2$, $n_F=80$, Landau level degeneracy $n_L=512$, and $q_l=2/l_B$. The fit is to a Gaussian of deviation Γ. Inset: dots are the numerical values of Γ for different cutoff wave vectors q_l, divided by the random matrix approximation Γ^{RMA} [Eq. (22)].

$$\mathcal{H}_0(t) = \frac{\hbar\omega_c}{2}|\boldsymbol{\pi} + \mathbf{a}(t)|^2. \tag{26}$$

The Schrödinger equation for the evolution operator,

$$i\hbar\partial_t U_F(t,t_0) = \mathcal{H}_0(t)U_F(t,t_0), \tag{27}$$

is solved in Appendix B and is given by

$$U_F(t,t_0) = e^{-i\boldsymbol{\xi}(t)\cdot\boldsymbol{\pi}}e^{-i\bar{\mathcal{H}}_0(t-t_0)}e^{+i\boldsymbol{\xi}(t_0)\cdot\boldsymbol{\pi}},$$

$$\bar{\mathcal{H}}_0(t) = \sum_{nk}\hbar n\omega_c|nk\rangle\langle nk|, \tag{28}$$

where the Floquet Hamiltonian $\bar{\mathcal{H}}_0$ is identical to the time independent Hamiltonian. This identity (called Kohn's theorem) also holds in the presence of arbitrary two-body interactions $\Sigma_{i<j}V(\mathbf{r}_i-\mathbf{r}_j)$ between electrons.[25]

The vector fields $\boldsymbol{\xi}(t)=\boldsymbol{\xi}_\omega+\boldsymbol{\xi}_0$ are solutions of coupled linear equations. Their explicit form, given in Appendix B, is well known,[14]

$$\xi_x^\omega = -\frac{el_B\omega_c}{\hbar\omega}\Re\left[\frac{\omega_c E_\omega^y + i\omega E_\omega^x}{\omega_c^2-\omega^2}e^{-i\omega t}\right],$$

$$\xi_y^\omega = \frac{el_B\omega_c}{\hbar\omega}\Re\left[\frac{\omega_c E_\omega^x - i\omega E_\omega^y}{\omega_c^2-\omega^2}e^{-i\omega t}\right],$$

$$\xi_0(t) = t\frac{el_B}{\hbar}\mathbf{E}_{dc}\times\hat{\mathbf{z}} - \frac{el_B}{\hbar\omega_c}\mathbf{E}_{dc}. \tag{29}$$

B. Floquet transformation with disorder

In Eq. (20), we have constructed the long range disorder operator $\mathcal{V}_l$ to a function only of $\mathbf{R}$. Thus, Eq. (13) implies the trivial, *yet very useful*, commutation relation

$$[\mathcal{V}_l, \boldsymbol{\pi}] = 0, \tag{30}$$

which we exploit to write the time dependent disordered Hamiltonian as

$$\mathcal{H}_d(t) = \mathcal{H}_0[\boldsymbol{\pi}, \mathbf{a}(t)] + \mathcal{V}_l[\mathbf{R}]. \tag{31}$$

Now, we can construct the *disordered Floquet evolution operator* U_d, which obeys the evolution equation

$$i\hbar\partial_t U_d(t,t_0) = \mathcal{H}_d(t)U_d(t,t_0). \tag{32}$$

Since the Floquet operators $e^{i\boldsymbol{\xi}(t)\cdot\boldsymbol{\pi}}$ commute with $\mathcal{V}_l[\mathbf{R}]$, the solution is simply

$$U_d(t,t_0) = e^{-i\boldsymbol{\xi}(t)\cdot\boldsymbol{\pi}}e^{-i\bar{\mathcal{H}}_d(t-t_0)}e^{+i\boldsymbol{\xi}(t_0)\cdot\boldsymbol{\pi}},$$

$$\bar{\mathcal{H}}_d = \sum_{n\alpha}(\hbar n\omega_c + \epsilon_\alpha)|n\alpha\rangle\langle n\alpha|, \tag{33}$$

with the same vector function $\boldsymbol{\xi}(t)$ as for the clean Landau level problem [Eq. (29)]. For $\mathbf{E}_{dc}=0$, the Floquet states $|n\alpha(t)\rangle=U^d(t,t_0)|n,\alpha\rangle$ return to themselves (up to a phase) at every integer period.

Expression (33) implies that the Floquet quasienergies (the spectrum of the transformed Hamiltonian $\bar{\mathcal{H}}_d$) are the *disorder broadened* Landau levels. The equivalence between stationary and quasistationary states with time dependent electric fields is a special property shared by harmonic oscillators, Landau levels, and our $\mathcal{H}_d$.

Using the last equation in Eq. (B3), we can also explicitly express the time dependent Fourier operator as

$$e^{i\mathbf{q}\cdot\mathbf{r}(t)} = e^{(i/\hbar)\bar{\mathcal{H}}_d t}e^{i\mathbf{q}\cdot\mathbf{r}}e^{-(i/\hbar)\bar{\mathcal{H}}_d t}e^{il_B\mathbf{q}\cdot\boldsymbol{\xi}(t)}, \tag{34}$$

where we can use the explicit solution [Eq. (29)] to perform the Bessel expansion,

$$e^{il_B\mathbf{q}\cdot\boldsymbol{\xi}(t)} = e^{-i\psi}\sum_{\nu=-\infty}^{\infty} i^\nu J_\nu(\tilde{q}\Delta_{\omega\hat{\mathbf{q}}})e^{it[\nu\omega+(el_B^2/\hbar)\mathbf{q}\times\mathbf{E}_{dc}\cdot\hat{\mathbf{z}}]}, \tag{35}$$

where ψ is an unimportant phase and J_ν is the Bessel function of order ν. The quantity

$$\Delta_{\omega\hat{\mathbf{q}}}(\mathbf{E}_\omega) \equiv \max_t[\hat{\mathbf{q}}\cdot\boldsymbol{\xi}(t)] \tag{36}$$

is proportional to the microwave field strength. For positive circular polarized light of field $\mathbf{E}_\omega=E_\omega^+(\hat{\mathbf{x}}+i\hat{\mathbf{y}})$, $\boldsymbol{\xi}$ and $\Delta_{\omega\hat{\mathbf{q}}}$ diverge at the cyclotron resonance as $|\omega-\omega_c|^{-1}$. For the opposite polarization, $\Delta_{\omega\hat{\mathbf{q}}}$ is continuous at resonance.

V. CALCULATION OF THE CURRENT

The dc current density is given by the full evolution operator U as

$$\mathbf{j} = \frac{e\hbar}{\mathcal{A}ml_B}\sum_{n\alpha}\rho_{n\alpha}\langle n\alpha|\overline{U^\dagger(t,t_0)\boldsymbol{\pi}U(t,t_0)+\mathbf{a}(t)}|n\alpha\rangle, \tag{37}$$

where $\rho_{n\alpha}$ is the electron density operator defined in the Floquet basis $|n,\alpha\rangle$.

The notation $\overline{F(t,t_0)}$ implies averaging the end-point times t,t_0 over many periods of $2\pi/\omega$.

A. Zeroth order theory

The zeroth order dc current density is given by setting $U \to U_d$ in Eq. (37). Using Eqs. (B3) and (29), it is easy to obtain

$$\mathbf{j}^{(0)} = (\boldsymbol{\xi}_0 \times \hat{\mathbf{z}} + \mathbf{a}_{dc}) \frac{e\hbar}{m l_B \mathcal{A}} \left(\sum_{n\alpha} \rho_{n\alpha} \right) = \frac{e^2 n_e}{m\omega_c} \hat{\mathbf{z}} \times \mathbf{E}_{dc}, \tag{38}$$

where the result holds for *any distribution* $\rho_{n\alpha}$ (not necessarily Fermi-Dirac) which sums up to the full electron density n_e.

It is interesting that although $\bar{\mathcal{H}}_d$ has random spectrum and wave functions, its current density [Eq. (38)] produces no dissipation. In addition, we see that the Hall conductivity is precisely given by the classical value

$$\sigma_H = \frac{e^2 n_e}{m\omega_c} = n_F \frac{e^2}{h}, \tag{39}$$

although for $\mathcal{V}_l \neq 0$, our system is by no means Galilean invariant. Incidentally, this result [Eq. (38)] applies in the presence of arbitrary electron-electron interactions which may be added to $\mathcal{H}_d(t)$.

We iterate that Eq. (38) applies only to the zeroth order Hamiltonian defined in Eq. (31). Dissipative effects enter at second order $\mathcal{O}(\mathcal{V}_s^2)$.

B. Second order dissipative current

The leading order dc current requires expanding the momentum operator to second order in $\mathcal{V}_s$. The interaction representation is defined as

$$\mathcal{O}^d(t,t_0) \equiv U_d^\dagger(t,t_0) \mathcal{O} U_d(t,t_0). \tag{40}$$

The zeroth order ("clean limit") Landau operator (in complex notation $\tilde{\boldsymbol{\pi}} = \boldsymbol{\pi}^x + i\boldsymbol{\pi}^y$) transforms as

$$\tilde{\boldsymbol{\pi}}^{(d)}(t,t_0) = e^{i\omega_c(t-t_0)} \tilde{\boldsymbol{\pi}} - \gamma(t,t_0), \tag{41}$$

where γ is an unimportant c-number function.

The full evolution operator U is expanded to second order in $\mathcal{V}_s$,

$$U(t,t_0) = U_d(t,t_0) \left[1 + \frac{-i}{\hbar} \int_{t_0}^{t} dt' \mathcal{V}_s(t',t_0) + \frac{(-i)^2}{\hbar^2} \int_{t_0}^{t} dt' \int_{t_0}^{t'} dt'' \mathcal{V}_s^d(t,t_0) \mathcal{V}_s^d(t'',t_0) + \cdots \right], \tag{42}$$

which yields the second order correction to the Landau operators as

$$\begin{aligned} \tilde{\boldsymbol{\pi}}^{(2)}(t,t_0) &= \frac{1}{\hbar^2} \int_0^t dt' \int_0^{t'} dt'' e^{i\omega_c(t-t_0)} \\ &\quad \times \left[[\tilde{\boldsymbol{\pi}}, \mathcal{V}_s^{(d)}(t',t_0)], \mathcal{V}_s^{(d)}(t'',t_0) \right] \\ &= \frac{1}{m l_B \hbar A^2} \sum_{\mathbf{q}\mathbf{q}'} V_{\mathbf{q}} V_{-\mathbf{q}'} (q_x + iq_y) \int_0^t dt' \int_0^{t'} dt'' e^{i\omega_c(t-t')} \\ &\quad \times \left[e^{i\mathbf{q}\cdot\mathbf{r}^{(d)}(t',t_0)}, e^{-i\mathbf{q}'\cdot\mathbf{r}^{(d)}(t'',t_0)} \right]. \end{aligned} \tag{43}$$

The leading order dissipative current is obtained by the disorder averaged expression

$$\mathbf{j}^d \simeq \frac{e\hbar}{\mathcal{A} m l_B} \left\langle \sum_{n\alpha} f_{n\alpha} \langle\langle n\alpha | \overline{\boldsymbol{\pi}^{(2)}(t,t_0)} | n\alpha \rangle\rangle_{\mathcal{V}_s} \right\rangle_{\mathcal{V}_l}. \tag{44}$$

Here, we use the Fermi-Dirac distribution

$$f_{n,\alpha} = (1 + e^{-E_{n\alpha}/T})^{-1}. \tag{45}$$

Corrections to the distribution function enter at higher order in $\mathcal{V}_s$ (see discussion in Sec. VII, item 2). Equation (44) ignores correlations between $\mathcal{V}_l$ and $\mathcal{V}_s$, which exist in the range $q < q_l$. The resulting error in the current, which is dominated by large wave vectors, is relatively suppressed by powers of q_l^2/q_s^2.

Using the matrix elements of the time dependent Fourier operator [Eq. (34)], we obtain

$$\begin{aligned} \langle n\alpha | e^{i\mathbf{q}\cdot\mathbf{r}^{(d)}(t,t_0)} | m\beta \rangle &= e^{(i/\hbar)(E_{n\alpha} - E_{m\beta})(t-t_0)} D_{nm}(\mathbf{q}) \\ &\quad \times \left[\sum_k e^{iq_x k l_B} \varphi_\alpha^*(k) \varphi_\beta(k + q_y l_B) \right] \\ &\quad \times \sum_{\nu=-\infty}^{\infty} J_\nu(\tilde{q}\Delta_{\omega\hat{\mathbf{q}}}) e^{it(\nu\omega + (el_B^2/\hbar)\mathbf{q}\times\mathbf{E}_{dc}\cdot\hat{\mathbf{z}})}. \end{aligned} \tag{46}$$

Averaging Eq. (43) over $\{V_{\mathbf{q}}\}$, keeping $\mathcal{V}_l$ fixed yields

$$\begin{aligned} \langle n\alpha | \tilde{\boldsymbol{\pi}}^{(2)}(t,t_0) | n\alpha \rangle_{\mathcal{V}_s} &= \frac{1}{\hbar \pi R_c A} \sum_{\mathbf{q}m} \frac{q_x + iq_y}{q} W(q) \\ &\quad \times (1 - \delta_{nm}\theta_{q<q_l}) I_{nm}(t,t_0), \end{aligned}$$

$$\begin{aligned} I_{nm}(t,t_0) &= \sum_{\alpha'} \int_0^{t-t_0} dt' e^{i\omega_c(t-t')} \\ &\quad \times \int_0^{t'} dt'' \frac{1}{2} \sum_{m\beta\pm} \pm e^{\pm i(E_{n\alpha} - E_{m\beta})(t'-t'')} \\ &\quad \times e^{i\mathbf{q}\cdot(\boldsymbol{\xi}(t'+t_0) - \boldsymbol{\xi}(t''+t_0))} |\langle \alpha | e^{i\tilde{\mathbf{q}}\cdot\mathbf{R}} | \beta \rangle|^2. \end{aligned} \tag{47}$$

We can henceforth neglect the terms $(-\delta_{nm}\theta_{q<q_l})$ in Eq. (47). The corrections contribute only to the low wave-vector integration and are therefore suppressed by factors of $(q_l/q_s) \ll 1$.

Integrating Eq. (44) over time, we obtain the full current expression

$$\begin{aligned} \mathbf{j}^d &\simeq \frac{e}{m R_c \omega_c} \int^{\pi k_F} \frac{d^2q}{(2\pi)^2} (\hat{\mathbf{z}} \times \mathbf{q}) \sum_{nm} \frac{W_{nm}^{res}(q)}{q} \\ &\quad \times \int d\epsilon d\epsilon' (f_{n,\epsilon} - f_{m,\epsilon'}) K_2(q,\epsilon,\epsilon') \\ &\quad \times \sum_\nu |J_\nu(\tilde{q}\Delta_{\omega\hat{\mathbf{q}}})|^2 \delta(E_{m\epsilon'} - E_{n\epsilon} - \hbar\nu\omega - el_B^2 \hat{\mathbf{z}} \times \mathbf{q} \cdot \mathbf{E}_{dc}), \end{aligned} \tag{48}$$

where K_2 is the disorder averaged intraband structure factor,

$$K_2(q,\epsilon,\epsilon') = \frac{1}{\mathcal{A}} \sum_{kk'\alpha\neq\beta} e^{i\tilde{q}_x(k-k')} \langle \varphi_\alpha^*(k)\varphi_\alpha(k')\varphi_\beta^*(k+\tilde{q}_y) \times \varphi_\beta(k'+\tilde{q}_y)\delta(\epsilon-\epsilon_\alpha)\delta(\epsilon'-\epsilon_\beta)\rangle_{\mathcal{V}_l}. \quad (49)$$

Note that by the symmetry of $\int d^2q$ integration, the second order current is parallel to the dc field and purely dissipative. Hence, to second order, the Hall conductivity *remains equal* to the classical value σ_H of Eq. (39).

C. Simplification at $T > \hbar\omega_c$

Many of the relevant experiments are carried out at temperatures $T > \hbar\omega_c$, where the Shubnikov–de Haas oscillations are thermally smeared. Using the energy-conserving delta function, we approximate the difference of Fermi functions as

$$f_{n,\epsilon} - f_{m,\epsilon'} \approx -\Theta(T-|\Delta E_\nu|)\Delta E_\nu \frac{\partial f(E_{n\epsilon})}{\partial E}, \quad (50)$$

where ΔE_ν is the transition energy,

$$\Delta E_\nu = \hbar\nu\omega + el_B^2\hat{\mathbf{z}}\times\mathbf{q}\cdot\mathbf{E}_{dc}. \quad (51)$$

Defining the single frequency structure factor K_1 as

$$K_1(q,\omega) = \int d\epsilon K_2(q,\epsilon,\epsilon+\hbar\omega), \quad (52)$$

the current expression simplifies to

$$j^d \simeq \frac{e}{4\pi^2 m v_F}\int^{\pi k_F} d^2q \frac{W(q)}{q}(\hat{\mathbf{z}}\times\mathbf{q}) \times \sum_{\nu,m}^{|\Delta E_\nu|\leq T} (\hbar\nu\omega + el_B^2\hat{\mathbf{z}}\times\mathbf{q}\cdot\mathbf{E}_{dc})|J_\nu(\tilde{q}\Delta_{\omega\hat{\mathbf{q}}})|^2 \times K_1(q, m\omega_c + \nu\omega + el_B^2\hat{\mathbf{z}}\times\mathbf{q}\cdot\mathbf{E}_{dc}/\hbar). \quad (53)$$

D. Random matrix approximation for the structure factors

Within the RMA, the Hamiltonian of each Landau level is taken as a member of the GUE. Thus, by the RMA, the wave functions $\varphi_\alpha(k)$ are normalized complex random vectors and the spectral correlations are completely uncorrelated beyond a few level spacings.[26] From random matrix theory, one has

$$\langle \varphi_\alpha^*(k)\varphi_\beta(k')\rangle_{\mathcal{V}} = \delta_{\alpha\beta}\delta_{kk'},$$

$$\frac{1}{\mathcal{A}^2}\left\langle \sum_{\alpha\beta}\delta(\epsilon-\epsilon_\alpha)\delta(\epsilon-\epsilon_\alpha)\right\rangle_{\mathcal{V}} = 2\pi l_B^2\rho(\epsilon)\rho(\epsilon'), \quad (54)$$

for $\epsilon-\epsilon' \gg \frac{\Gamma}{n_L}$. The RMA approximates the dynamical structure factor [Eq. (49)] as

$$K_2^{RMA}(\epsilon,\epsilon') = \frac{1}{(2\pi)^2 l_B^2\Gamma^2}\exp\left[-\frac{\epsilon^2+(\epsilon')^2}{2\Gamma^2}\right], \quad (55)$$

where $\Gamma = \Gamma^{RMA}$ is the width of the single Landau level density of states [Eq. (22)].

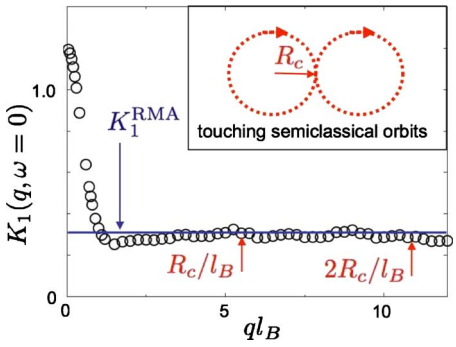

FIG. 5. (Color online) The static structure factor $K_1(q,\omega=0)$ evaluated numerically for $n_L=128$, $n_F=15$, and $q_l=1/l_B^2$. The exact correlator has a peak at zero wave vector of width q_l and agrees with the (wave vector independent) RMA at higher wave vectors. The inset depicts *classical* cyclotron orbits, which strongly overlap when separated by $2R_c$. In contrast, K_1 shows no signature of enhanced scattering at wave vectors corresponding to $2R_c$.

The RMA for the single frequency structure factor is

$$K_1^{RMA}(\omega) = \int d\epsilon K_2^{RMA}(\epsilon,\epsilon+\hbar\omega) = \frac{\sqrt{\pi}}{(2\pi)^2 l_B^2\Gamma}\exp\left(-\frac{\hbar^2\omega^2}{4\Gamma^2}\right). \quad (56)$$

We have computed the structure factor $K_1(q,\omega)$ numerically for a finite Landau level degeneracy on a cylinder. As depicted in Figs. 5 and 6, the RMA works well for $q \gg q_l$, where Γ is given by Eq. (25). This finding confirms our expectation that the RMA is applicable at large wave vectors since correlations between matrix elements of $V_{kk'}^{n_F}$ decay beyond the wave-vector scale $\tilde{q}_l$. In contrast, at low wave vectors $q \leqslant 3q_l$, there is a peak in K_1, which is absent in the RMA. It contributes negligibly, however, to the overall current. We note that there is no signature of enhanced scattering at wave vectors corresponding to the classical cyclotron diameter $2R_c$ (see discussion in Sec. VII, item 6).

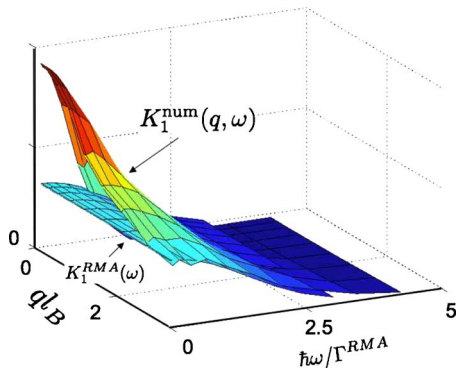

FIG. 6. (Color online) The dynamical structure factor. $K_1^{\mathrm{num}}(q,\omega)$ is evaluated numerically, for $n_L=64$, $n_F=80$, and $q_l=1/l_B$. The random matrix approximation K_1^{RMA} is given in Eq. (56). Good agreement is found for $q>3q_l$, at all frequencies.

VI. ANALYTICAL RESULTS

The full nonlinear current $\mathbf{j}^d(\mathbf{E}_{dc},\mathbf{E}_\omega,\omega,B,T,n_e)$ can be computed from Eq. (48), by numerically averaging K_1 over disorder. It is useful, however, to use the RMA and obtain analytical results. These allow a better understanding of the important characteristic energy and field scales of the nonlinear current.

The first order of business is to extract the dark linear conductivity from Eqs. (53) and (56). We obtain

$$\sigma_{xx}^{\text{dark}} = \frac{n_F e^2}{h}\left(\frac{\hbar}{2\pi^{1/2}\tau_{tr}\Gamma}\right). \tag{57}$$

Not surprisingly, this result agrees with the SCBA,[28] where the *transport scattering rate* is defined in the standard way:[23]

$$1/\tau_{tr} \equiv (2\pi\hbar^2 v_F k_F^2)^{-1}\int_0^{q_s} dq q^2 W(q). \tag{58}$$

Using the RMA for K_1, given by Eq. (56), the current can be simplified into an analytical expression

$$j^d = \sigma_{xx}^{\text{dark}} E_\Gamma\left[\varepsilon_{dc}F(\varepsilon_{dc},\varepsilon_\omega,\omega) + \left(\frac{\hbar\omega}{\Gamma}\right)G(\varepsilon_{dc},\varepsilon_\omega,\omega)\right]. \tag{59}$$

The dimensionless fields are defined as

$$\varepsilon_{dc} \equiv E/E_\Gamma,$$

$$\varepsilon_\omega \equiv \Delta_{\omega\hat{\mathbf{q}}_s} q_s l_B. \tag{60}$$

The characteristic electric field scale,

$$E_\Gamma = \Gamma/(e l_B^2 q_s), \tag{61}$$

defines the lowest scale of nonlinearity in j^d.

At $|\mathbf{E}| \approx E_\Gamma$, resonant intraband transitions are enabled over a distance of $l_B^2 q_s$.

For a white-noise short range disorder $W(q)=W_s\theta_{q<q_s}$, the dimensionless functions F,G in Eq. (59) are explicitly evaluated as

$$F = \frac{3}{\pi}\sum_{m\nu}^{|\Delta E_\nu|\le T}\int_{r\le 1} d^2 r \frac{y^2}{r}|J_\nu(r\varepsilon_\omega)|^2 e^{-[y\varepsilon_{dc}+\hbar(\nu\omega - m\omega_c)/\Gamma]^2/4},$$

$$G = \frac{3}{\pi}\sum_{m\nu}^{|\Delta E_\nu|\le T}\nu\int_{r\le 1} d^2 r \frac{y}{r}|J_\nu(r\varepsilon_\omega)|^2 e^{-[y\varepsilon_{dc}+\hbar(\nu\omega - m\omega_c)/\Gamma]^2/4}, \tag{62}$$

where the sums are limited by the temperature condition on the transition energies [Eq. (51)].

A. Microwave induced resistance oscillation: Photoconductivity oscillations

G describes the photocurrent contributions. Near a particular primary ($\nu=1$) resonance at some interband interval $\bar{m}\gg 1$, the dimensionless detuning frequency is defined as

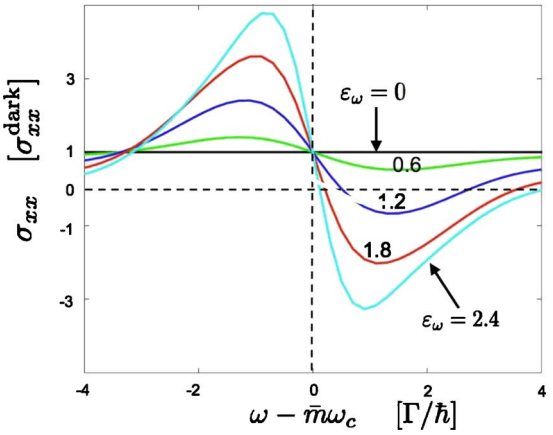

FIG. 7. (Color online) MIRO effect. The frequency dependent conductivity is plotted against the detuning frequency near the $\bar{m}$th resonance. A set of dimensionless microwave field strengths ε_ω is given. The broadening ratio [Eq. (65)] is chosen at $R=10$. Temperature is $T=7\hbar\omega_c$. The regions of negative conductivity are unstable toward the zero resistance state.

$$\delta_\omega = \frac{\hbar}{\Gamma}(\omega - \bar{m}\omega_c). \tag{63}$$

The MIRO effect, arising from the function G, changes sign at the resonances as

$$G \propto -\delta_\omega. \tag{64}$$

The magnitude of MIRO is controlled by the figure of merit, the Landau level broadening ratio

$$R \equiv \frac{\hbar\omega_c}{\Gamma} = \left(B\frac{2\pi^2\hbar^2 v_F e}{W_l q_l mc}\right)^{1/2}. \tag{65}$$

For $R\gg 1$, the total current at $\delta_\omega > 0$ can become negative and produce the zero resistance state. This ratio increases as $\sqrt{B}$. Our approximations, however, break down at low filling factors.

In Fig. 7, we plot a low field conductivity oscillation as a function of detuning frequency. We choose $R=10$ as the broadening ratio and a set of microwave radiation field strengths ε_ω. At temperature $T=7\hbar\omega_c$, we note that the conductivity at $\delta_\omega=0$ is independent of radiation power. The regions of negative conductivity are unstable to the formation of a ZRS.

B. Hall induced resistivity oscillation: The dark nonlinear current

In the absence of radiation, G vanishes and the nonlinear conductivity in Eq. (59) is $\sigma_{xx}^{\text{dark}}F$. In Fig. 8, we plot $F(E)$ for different values of $\hbar\omega_c/\Gamma$.

At weak fields of order E_Γ, we see a Gaussian decrease of conductivity due to diminishing phase space for intra-Landau band scattering. Caution has to be exercised in trying to fit the low conductivity regime with Eq. (48). The far tails of the density of states require multiple scattering theory, which goes far beyond second order in $\mathcal{V}_s$.[29]

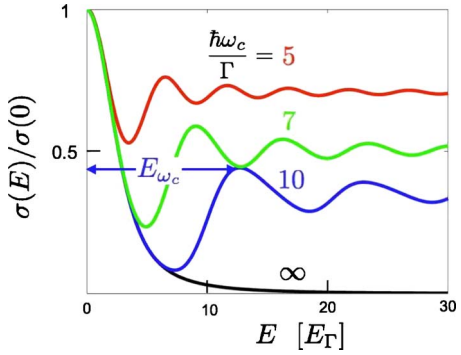

FIG. 8. (Color online) The HIRO effect. Nonlinear current oscillations at zero radiation, as a function of dc electric field, for a set of broadening ratios R. The field scale E_Γ is defined in Eq. (61). The oscillation periodicity is determined by $E_{\omega_c}=RE_\Gamma$.

At larger fields, the conductivity has secondary maxima at

$$|\mathbf{E}^{max}| = (m+\delta)E_{\omega_c}, \quad \delta \approx 0.25, m = 1,2,\ldots,$$

$$E_{\omega_c} = \frac{\hbar\omega_c}{el_B^2 q_s} = RE_\Gamma, \tag{66}$$

which corresponds to the inter-Landau level scattering over the length scale $q_s l_B^2$. For $q_s > \pi k_F$, by Eq. (A4), one must use $q_s \to k_F \pi$.

C. Nonlinear photocurrent and zero resistance state fields

In Fig. 9, we plot the fully irradiated nonlinear current at different microwave fields, at one fixed optimal detuning of $\delta_\omega=0.9$. For weak radiation, the HIRO oscillations are observed, and their phase shifts as the microwave power increases. At stronger radiation, the negative conductivity regions are unstable toward the ZRS. The ZRS creates spontaneous electric fields of magnitude E^{zrs}, where the dissipative current vanishes $j^d(E^{zrs})=0$.[11,12] In Fig. 10, we plot the dependence of $E^{zrs}(\varepsilon_\omega)$ at fixed detuning frequency. The

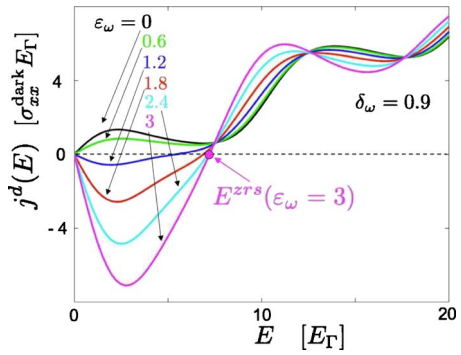

FIG. 9. (Color online) Nonlinear current-field characteristics for different levels of microwave field ε_ω. The field scale is E_Γ (Eq. (61)). Temperature is chosen at $T=7\hbar\omega_c$ and the broadening ratio is $R=10$. δ_ω, defined in Eq. (63), is fixed at 0.9. Negative current regimes are unstable to a ZRS with spontaneous electric fields of magnitude E^{zrs}.

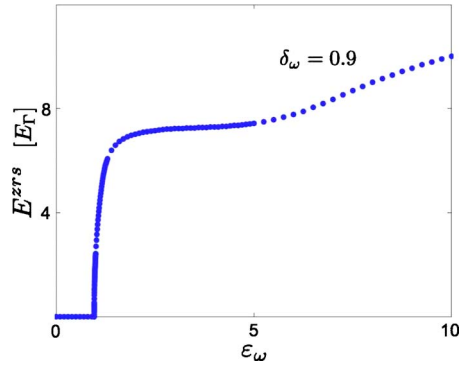

FIG. 10. (Color online) The ZRS spontaneous field. E^{zrs} is given by the zero of $j^d(E)$ as a function of dimensionless microwave field ε_ω, at fixed detuning frequency δ_ω. A continuous (second order) dynamical transition occurs at a threshold microwave field.

ZRS exhibits a continuous dynamical phase transition as a function of microwave power, which was previously predicted on phenomenological grounds, by Alicea *et al.*[30]

VII. DISCUSSION

We emphasize several issues regarding our results.

(1) Our analysis is limited to second order in the short range disorder $\mathcal{V}_s$, which is controlled by the smallness of $W_s q_s/(W_l q_l) < 1$. In physical terms, this is equivalent to the well known "small angle scattering" limit where $\hbar/(\tau_{tr}\Gamma) < 1$, with Γ and τ_{tr} defined by Eqs. (25) and (58), respectively. Small angle scattering is used to justify the SCBA.[22] By Eqs. (39) and (57), the small angle scattering parameter can be *experimentally* determined by the Hall angle θ_H,

$$\cot(\theta_H) = \frac{\sigma_{xx}^{\text{dark}}}{\sigma_H} = \left(\frac{\hbar}{2\pi^{1/2}\tau_{tr}\Gamma}\right). \tag{67}$$

By Eq. (7), a large Hall angle $\theta_H \approx \pi/2$ is also the limit which effectively separates the effects of dissipative and Hall fields in the Hall bar geometry.[6,7]

(2) Our photoconductivity supports the displacement photocurrent mechanism.[14,15] We have assumed here that electron-electron interactions are relatively weak for well resolved high Landau levels. However, we also implicitly assume that electron-phonon interactions are strong enough to produce an inelastic scattering time of the order

$$\tau_{in} \approx \tau_{tr}. \tag{68}$$

Hence, to the leading order in $1/\tau_{tr}$, we do not need to correct the Fermi-Dirac distribution. We do not rule out that the DF mechanism[18] may yield sizable corrections, for the case $\tau_{in} > \tau_{tr}$.

(3) We have assumed a model of weak disorder which produces *well separated* Landau levels. We find that a large ratio $\hbar\omega_c/\Gamma$ can produce large MIRO and ZRS effects under radiation. It is also responsible for a large HIRO effect. Indeed, these effects have been observed in the same samples.[10]

(4) The conductivity at $\omega=m\omega_c$ appears to be insensitive to the radiation field (see Fig. 7). Within Eq. (59), this is true

only at temperatures $T/(\hbar\omega_c)=\nu^{max}\gg 1$; otherwise, the Bessel function sum rule,

$$\lim_{\nu^{\max}\to\infty}\sum_{|\nu|\le\nu^{\max}}|J_\nu(r\varepsilon_\omega)|^2=1, \tag{69}$$

is not saturated. At very low temperatures, only a few Bessel functions contribute, and we expect the conductivity at resonance frequencies to be suppressed under radiation.

(5) The characteristic field E_Γ [Eq. (61)] is in the same ball park as Ryzhii's estimate.[14] It differs from the much larger estimate $[\gtrsim\hbar\omega_c/(eR_c)]$ provided by Ref. 19.

(6) The characteristic field of secondary HIRO maxima [Eq. (66)] depends on the disorder cutoff q_s. This is in contrast to the semiclassical picture[6] of touching cyclotron orbits of radii $R_c=v_F/\omega_c$. This scenario is depicted in the inset of Fig. 5. This argument suggests an enhanced scattering at an electric field

$$E_{2R_c}=\frac{\hbar\omega_c}{2eR_c}\neq E_{\omega_c}, \tag{70}$$

where our E_{ω_c} in Eq. (66) depends on q_s. As evidenced in Figs. 3 and 5, there is no signature of enhanced scattering at wave vectors $2R_c/l_B^2$, unless, by coincidence, the short range cutoff precisely matches $q_s=2k_F$. In summary, the cyclotron radius is not a noticeable length scale in the structure factor at high Landau levels.

Experimentally,[8] values of oscillation field have *not* been universal and have varied in the range $(1.63,2.18)\times E_{2R_c}$.

(7) An important issue, which we have ignored in this work, is the relation between the dimensionless microwave field ε_ω and an external microwave radiation field and polarization. The resonance of positive circular polarization at $\omega=\omega_c$ implies that close to the cyclotron resonance, one cannot ignore the strong frequency and polarization dependence of the dielectric function. There are related open issues raised by recent experiments, most notably the apparent independence of the MIRO on the microwave polarization[31] and the seeming inability of two photon absorption to explain a MIRO about $\omega_c/2$.[32] We shall defer discussion of these problems to further investigations.

ACKNOWLEDGMENTS

We thank Igor Aleiner, Herb Fertig, Shmuel Fishman, Leonid Glazman, Bert Halperin, Misha Raikh, Boris Shklovskii, Amir Yacoby, and Michael Zudov for informative discussions. We acknowledge support from the Israel Science Foundation, the U.S.-Israel Binational Science Foundation, and the fund for Promotion of Research at Technion. A.A. is grateful for the hospitality of Aspen Center for Physics.

APPENDIX A: THE DISORDER MATRIX ELEMENTS

Using the definition [Eq. (12)], the commutation between Landau operators and guiding center coordinates are readily obtained, for $\alpha,\beta=x,y$,

$$[\pi_\alpha,R_\beta]=0,$$

$$[\pi_x,\pi_y]=[R_y,R_x]=i. \tag{A1}$$

The full disorder operator is expressed as

$$\mathcal{V}=\frac{1}{\mathcal{A}}\sum_{\mathbf{q}}V_{\mathbf{q}}e^{-il_B\mathbf{q}\cdot\boldsymbol{\pi}\times\hat{\mathbf{z}}}e^{-il_B\mathbf{q}\cdot\mathbf{R}}. \tag{A2}$$

The matrix elements of the Fourier operators are given by

$$\langle k|e^{-il_B\mathbf{q}\cdot\mathbf{R}}|k'\rangle=e^{-iq_xkl_B}\delta_{k',k+q_yl_B},$$

$$\begin{aligned}\langle n|e^{-il_B\mathbf{q}\cdot\boldsymbol{\pi}\times\hat{\mathbf{z}}}|m\rangle&=e^{-(ql_B)^2/4}|\mathbf{q}l_B/\sqrt{2}|^{(m-n)}e^{i(m-n)\phi}\\&\times\sqrt{\frac{m!}{n!}}L_n^{m-n}[(ql_B)^2/2]\\&\equiv D_{nm}(\mathbf{q}),\end{aligned} \tag{A3}$$

where $\phi=\arctan(q_y/q_x)$. Equation (A3) is used to split the long and short wavelength terms in $\mathcal{V}$ in Eqs. (21) and (48).

The asymptotic expression for the associated Laguerre polynomials[33] valid at large $n<m$, with $\tilde{q}=ql_B<\sqrt{2n}\pi$, yields

$$\tilde{q}|D_{nm}(\tilde{q}^2/2)|^2\sim\frac{2}{\sqrt{2n}\pi}\cos^2(\sqrt{2n}\tilde{q}-\phi_{n-m}), \tag{A4}$$

where $\phi=\pi/4+\pi(m-n)/2$. The fast oscillations of the $\cos^2$ can be replaced by its constant average of $\frac{1}{2}$, which simplifies the q integration over smooth functions considerably.

APPENDIX B: THE EXPLICIT FLOQUET OPERATOR

The full disordered evolution operator [Eq. (28)] is decomposed into

$$U_F(t,t_0)=W(t)\exp\left[-\frac{i}{\hbar}\bar{\mathcal{H}}_0(t-t_0)\right]W^\dagger(t_0), \tag{B1}$$

where $\bar{\mathcal{H}}_0$ is the clean Landau level Hamiltonian, and the vector-potential-dependent Floquet operator W is defined as

$$W(t)=e^{-i\boldsymbol{\xi}(t)\cdot\boldsymbol{\pi}}e^{-i\int^t L(t')dt'}. \tag{B2}$$

Here, we shall determine the fields $\boldsymbol{\xi}(t),L(t)$. W acts on the time derivative and translates the Landau level coordinates $\boldsymbol{\pi}$ as follows:

$$W^\dagger(i\partial_t)W=(i\partial_t)+\boldsymbol{\pi}\cdot\dot{\boldsymbol{\xi}}+\frac{1}{2}\partial_t(\xi_x\xi_y)+L(t),$$

$$W^\dagger\boldsymbol{\pi}W=\boldsymbol{\pi}+\boldsymbol{\xi}\times\hat{\mathbf{z}},$$

$$W^\dagger\mathbf{r}W=\mathbf{r}+l_B\boldsymbol{\xi}, \tag{B3}$$

which transforms the evolution equation as

$$W^{\dagger}\left(i\partial_t - \frac{\omega_c}{2}|\boldsymbol{\pi}+\mathbf{a}|^2\right)W = i\partial_t - \frac{\omega_c}{2}|\boldsymbol{\pi}+\boldsymbol{\xi}\times\hat{\mathbf{z}}+\mathbf{a}-\dot{\boldsymbol{\xi}}/\omega_c|^2 + \frac{|\dot{\boldsymbol{\xi}}|^2}{2\omega_c} + \frac{1}{2}(\xi_x\xi_y) + L(t) = i\hbar\partial_t - \bar{\mathcal{H}}_d. \tag{B4}$$

The fields $\boldsymbol{\xi}$ are given by solving the linear equations

$$\dot{\boldsymbol{\xi}} - \omega_c\boldsymbol{\xi}\times\hat{\mathbf{z}} = \omega_c\mathbf{a}(t),$$

$$L(t) = \frac{1}{2}(\xi_x\xi_y). \tag{B5}$$

For convenience, we fix the origin of time $t=0$, such that $\boldsymbol{\xi}(t=0)=\boldsymbol{\xi}_0$.

Using the complex notation $\tilde{\xi}=\xi_x+i\xi_y$, we write

$$\dot{\tilde{\xi}} + i\omega_c\tilde{\xi} = \omega_c\tilde{a}(t). \tag{B6}$$

The dimensionless gauge field (written in circular polarized components) is

$$\tilde{a} = a_x + ia_y = \frac{el_B}{\hbar}\left(\frac{iE_\omega^+}{\omega}e^{-i\omega t} - \frac{iE_\omega^-}{\omega}e^{i\omega t} + \tilde{E}_{dc}t\right). \tag{B7}$$

Separating the solution into $\tilde{\xi}(t)=\tilde{\xi}^+ + \tilde{\xi}^- + \tilde{\xi}_0$, one obtains

$$\tilde{\xi}^{\pm} = \pm\frac{el_B\omega_c}{\hbar\omega}\frac{E_\omega^{\pm}}{\omega_c \mp \omega}e^{\mp i\omega t},$$

$$\tilde{\xi}_0 = -i\frac{el_B\tilde{E}_{dc}}{\hbar}t - \frac{el_B\tilde{E}_{dc}}{\hbar\omega_c}. \tag{B8}$$

The zero frequency component of $\boldsymbol{\xi}$ in Cartesian coordinates is

$$\boldsymbol{\xi}_0(t) = t\frac{el_B}{\hbar}\mathbf{E}_{dc}\times\hat{\mathbf{z}} - \frac{el_B}{\hbar\omega_c}\mathbf{E}_{dc}. \tag{B9}$$

In vector notation, we thus derived the explicit form of the Floquet fields $\boldsymbol{\xi}(t)$ as given in the main text by Eq. (29).

[1] R. G. Mani, J. H. Smet, K. von Klitzing, V. Narayanamurti, W. B. Johnson, and V. Umansky, Nature (London) **420**, 646 (2002).
[2] M. A. Zudov, R. R. Du, J. A. Simmons, and J. R. Reno, Phys. Rev. B **64**, 201311(R) (2001).
[3] P. D. Ye, L. W. Engel, D. C. Tsui, J. A. Simmons, J. R. Wendt, G. A. Vawter, and J. L. Reno, Appl. Phys. Lett. **79**, 2193 (2001).
[4] M. A. Zudov, R. R. Du, L. N. Pfeiffer, and K. W. West, Phys. Rev. Lett. **90**, 046807 (2003).
[5] S. A. Studenikin, M. Potemski, A. Sachrajda, M. Hilke, L. N. Pfeiffer, and K. W. West, Phys. Rev. B **71**, 245313 (2005).
[6] C. L. Yang, J. Zhang, R. R. Du, J. A. Simmons, and J. L. Reno, Phys. Rev. Lett. **89**, 076801 (2002).
[7] A. A. Bykov, J. Q. Zhang, S. Vitkalov, A. K. Kalagin, and A. K. Bakarov, Phys. Rev. B **72**, 245307 (2005).
[8] W. Zhang, H.-S. Chiang, M. A. Zudov, L. N. Pfeiffer, and K. W. West, Phys. Rev. B **75**, 041304(R) (2007).
[9] J-q. Zhang, S. Vitkalov, A. A. Bykov, A. K. Kalagin, and A. K. Bakarov, Phys. Rev. B **75**, 081305(R) (2007).
[10] W. Zhang, M. A. Zudov, L. N. Pfeiffer, and K. W. West, Phys. Rev. Lett. **98**, 106804 (2007).
[11] A. V. Andreev, I. L. Aleiner, and A. J. Millis, Phys. Rev. Lett. **91**, 056803 (2003).
[12] A. Auerbach, I. Finkler, B. I. Halperin, and A. Yacoby, Phys. Rev. Lett. **94**, 196801 (2005).
[13] I. Finkler, B. I. Halperin, A. Auerbach, and A. Yacoby, J. Stat. Phys. **125**, 1097 (2006).
[14] V. I. Ryzhii, Fiz. Tverd. Tela (Leningrad) **11**, 2577 (1969) [Sov. Phys. Solid State **11**, 2078 (1970)]; V. Ryzhii and V. Vyurkov, Phys. Rev. B **68**, 165406 (2003); V. I. Ryzhii, Jpn. J. Appl. Phys., Part 1 **44**, 6600 (2005).
[15] A. C. Durst, S. Sachdev, N. Read, and S. M. Girvin, Phys. Rev. Lett. **91**, 086803 (2003).
[16] X. L. Lei and S. Y. Liu, Phys. Rev. Lett. **91**, 226805 (2003).
[17] M. Torres and A. Kunold, Phys. Rev. B **71**, 115313 (2005); J. Phys.: Condens. Matter **10**, 4029 (2006); J. Iñarrea and G. Platero, Phys. Rev. Lett. **94**, 016806 (2005).
[18] I. A. Dmitriev, M. G. Vavilov, I. L. Aleiner, A. D. Mirlin, and D. G. Polyakov, Phys. Rev. B **71**, 115316 (2005).
[19] M. G. Vavilov and I. L. Aleiner, Phys. Rev. B **69**, 035303 (2004).
[20] T. Ando and Y. Uemura, J. Phys. Soc. Jpn. **36**, 959 (1974).
[21] The SCBA result for $\sigma^{xx}\propto(\tau_s/\tau_{tr})$ (Ref. 22) demonstrates that perturbation theory about a clean system is singular in the long wavelength disorder.
[22] M. E. Raikh and T. V. Shahbazyan, Phys. Rev. B **47**, 1522 (1993).
[23] Our approach was inspired by the study of MIRO effect in the presence of a large periodic potential: J. Dietel, L. I. Glazman, F. W. Hekking, and F. von Oppen, Phys. Rev. B **71**, 045329 (2005).
[24] A. L. Efros, F. G. Pikus, and G. G. Samsonidze, Phys. Rev. B **41**, 8295 (1990).
[25] W. Kohn, Phys. Rev. **123**, 1242 (1961).
[26] M. L. Mehta, *Random Matrices* (Academic, New York, 1991).
[27] C. W. J. Beenakker, Rev. Mod. Phys. **69**, 731 (1997).
[28] Equation (57) is smaller by a factor of $\sqrt{\pi}/4$ than the dark conductivity of the SCBA (Ref. 20), which is probably due to the different form of density of states tails.
[29] M. M. Fogler, A. Yu. Dobin, and B. I. Shklovskii, Phys. Rev. B **57**, 4614 (1998).
[30] J. Alicea, L. Balents, M. P. A. Fisher, A. Paramekanti, and L. Radzihovsky, Phys. Rev. B **71**, 235322 (2005).
[31] J. H. Smet, B. Gorshunov, C. Jiang, L. Pfeiffer, K. West, V. Umansky, M. Dressel, R. Meisels, F. Kuchar, and K. von Klitzing, Phys. Rev. Lett. **98**, 219902(E) (2007).
[32] S. I. Dorozhkin, J. H. Smet, K. von Klitzing, L. N. Pfeiffer, and K. W. West, arXiv:cond-mat/0608633 (unpublished).
[33] I. S. Gradshteyn and I. M. Ryzhik, *Table of Integrals, Series and Products* (Academic, New York, 1980), p. 1039.